New Journal of Physics
The open access journal for physics

Weak localization of photon noise

Paolo S Scalia[1,3], **Otto L Muskens**[2] **and Ad Lagendijk**[1]

[1] FOM-Institute AMOLF, Science Park 104, 1098-XG Amsterdam, Netherlands
[2] Physics and Astronomy, Faculty of Physical and Applied Sciences, University of Southampton, Highfield, Southampton SO17 1BJ, UK
E-mail: p.s.scalia@gmail.com

New Journal of Physics **15** (2013) 105009 (12pp)
Received 30 May 2013
Published 8 October 2013
Online at http://www.njp.org/
doi:10.1088/1367-2630/15/10/105009

Abstract. We present an experimental study of coherent backscattering (CBS) of photon noise from multiple scattering media. We use a pseudothermal light source with a microsecond coherence time to produce a noise spectrum covering a continuous transition, from wave fluctuations to shot noise over several MHz. The angle-dependent Fano factor of backscattered light shows an enhancement due to CBS in the wave fluctuation regime. The CBS line shape and enhancement factor of the noise power is consistent with theory in the weak-scattering limit and for a large number of open reflection channels. These initial experiments on weakly scattering media demonstrate that sensitive noise measurements can be combined with the separation of path lengths present in CBS, opening up new experiments on noise transport in the localization regime.

Contents

[3] Author to whom any correspondence should be addressed.

1. Introduction

Propagation of coherent light through multiple scattering media gives rise to a rich variety of phenomena of fundamental interest: Anderson localization, coherent backscattering (CBS), random lasing and different types of correlations are among the most well known examples [1–10]. Considerable theoretical as well as experimental effort has been focused on the transport of noise in chaotic and diffusive electronic systems, and the transition from classical to quantum states has raised particular interest [11–13]. Recently, the propagation of optical noise in strongly scattering systems has received much attention. Pioneering work has been reported that investigates multiple light scattering in the regime of quantum optics [14–22]. Deviations from Poissonian statistics have been found when light in the coherent state propagates through moving scatterers [23].

Photonic systems are crucial to the development of fast data communication protocols as they outperform electronic systems with respect to data capacity [24]. Furthermore, several studies have suggested how multiple scattering can be exploited to enhance information transfer [25, 26]. The ultimate barrier to optical information transfer is photon shot noise which is quantum in essence [27, 28], as it is due to the granular nature of light. Despite having been known and studied for a long time, only recently classical laser noise has been reported as the fastest physical mean to generate random numbers [29, 30], opening the way for novel methods to yield security key codes at high speeds.

The goal of the experiments presented in this paper is to extend the study of photon noise to a CBS configuration. CBS results from interference effects between reciprocal paths in a random medium, and manifests itself as a twofold enhancement of the light intensity in the backscattering direction with respect to the diffuse background. Measurements of CBS have turned over the years from a striking evidence of weak localization of light to a tool for investigating the scattering properties of many different media [31–33]. The strong Anderson localization transition has received much attention since it was first proposed in 1958 [34], nevertheless it remains an elusive phenomenon for light in three-dimensional (3D) media [8, 9, 35, 36]. Noise measurements could provide an alternative means to investigate the critical regime near localization. In this paper we present the first experimental investigation of weak localization of photon shot noise and pseudothermal noise from scattering media.

2. Optical setup and sample

The basic elements to induce and measure photon noise are depicted in figure 1. In order to achieve sufficient intensity we use a Ti:Sa laser which is operated in cw mode, at a wavelength of 780 nm with an output power of 1.6 W. The laser output was shot-noise limited at frequencies above several hundred kHz. Pseudothermal light was generated by focusing the laser output beam onto a rotating diffuser. The ground glass diffuser is schematized in figure 1 as a collection of random glass defects called microareas. The laser beam is randomly scattered by the microareas. The diffuser rotates, therefore the incoming beam illuminates different microareas, that in turn act like independent sources. By independent it is meant that there is no phase relationship among fields produced by different microareas. This is the key property that makes a ground glass diffuser a pseudothermal source: the microareas mimic the behavior of the emitting atoms of molecules in a true thermal source. By spinning the diffuser it was

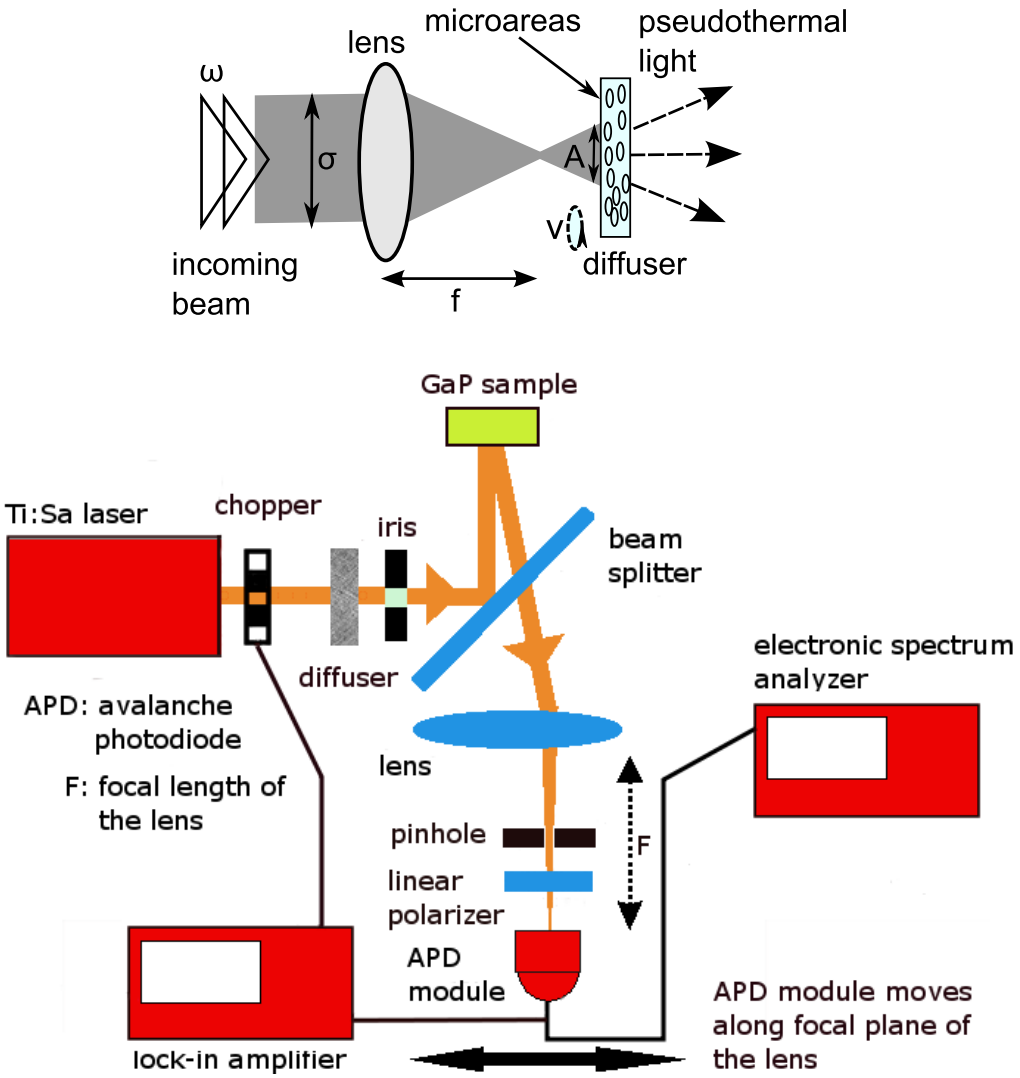

Figure 1. (top) Setup consisting of a lens and a diffuser used to generate pseudothermal light. A laser beam of frequency ω and diameter σ is focused by a lens of focal lens f and impinges on a ground glass diffuser rotating at speed v. With A is indicated the cross section of the beam on the diffuser. The ground glass diffuser is modeled as a collection of random microareas. The rotation of the microareas gives rise to pseudothermal light. (bottom) Schematic overview of the experimental setup for measurement of noise and intensity CBS. A polarizer (not shown) is placed before the beam splitter to select the incoming polarization.

possible to introduce excess noise up to the MHz regime. The pseudothermal light source was integrated into a CBS set up as shown in the bottom scheme of figure 1.

CBS of both intensity and noise is measured in a beamsplitter configuration [2]. Light scattered from the sample was collected by a lens ($f = 8$ cm) and detected by an avalanche photodiode (APD) module (Hamamatsu C4777) that moved along the focal plane of the lens. An electronic spectrum analyzer (Agilent) was used to measure the noise power spectrum. The angular resolution amounted to 1.2 mrad and was determined by a 100 μm pinhole placed in

front of the detector. The sample was slightly tilted to prevent light which was specularly reflected from the sample to be detected. Speckle averaging was obtained by rotating the sample around its azimuthal axis using a spinning motor. Polarization filters were used to individually select polarization conserving and non-conserving backscattering channels. Lock-in detection minimizes the influence of stray light. For the CBS experiments we used a strongly scattering slab of porous GaP fabricated via an electrochemical etching technique, and showing negligible absorption at 780 nm [37]. The slab has thickness $L \simeq 70\,\mu$m and a photonic strength $k_0\ell_B = 17.7$, where ℓ_B denotes the (Boltzmann) mean free path of light inside the scattering medium and k_0 is the free-space wavevector of the light. Noise spectra were acquired using the spectrum analyzer with a resolution bandwidth of 30 kHz and a video bandwidth of 10 kHz over a frequency segment that spans 8.85 MHz, from 0.15 to 10 MHz. Each point in the noise traces presented here was obtained by computing the average of 50 consecutive points in the spectrum. Intensity and noise CBS-cones were normalized to the intensity and noise power measured in the polarization non-conserving channel, respectively.

Noise spectra as function of angle and frequency and cross sections at different frequencies are shown in figure 2 (top panel). The data highlight how the CBS shape changes from the shot noise regime at frequencies above 5 MHz to the pseudothermal noise regime at low frequencies below 5 MHz. In addition to the CBS noise cones at different frequencies, we have plotted the CBS intensity cone and its square in figure 2 (bottom panel) for three different frequencies. In order to compare the shapes of the three cones, they were normalized to their value assumed on the left most angle. The comparison to the intensity data shows how the shot noise cone, obtained from the high-frequency data, follows closely the intensity cone whereas the intensity CBS cone squared is an upper bound for the pseudothermal cones, which are obtained for the low-frequency data. The enhancement of the noise produced by pseudothermal light exceeds the ordinary maximum value of 2 obtainable for the intensity cone, this is due to the different functional dependences that shot noise and pseudothermal noise display with respect to the intensity, as it will be shown in section 3.

3. Model

The noise power spectrum $S(\Omega)$ needs to be calculated to model the experiment and is given by

$$S(\Omega) = \int_{-\infty}^{+\infty} \langle \hat{j}(t)\,\hat{j}(t+\tau)\rangle \exp\left(-\mathrm{i}\Omega\tau\right)\,\mathrm{d}\tau, \tag{1}$$

where Ω denotes the noise frequency, $\hat{j}(t)$ the photocurrent operator and with $\langle\rangle$ we indicate quantum averaging. Making use of the quantum derivation used in [38] it follows that

$$\langle \hat{j}(t)\,\hat{j}(t+\tau)\rangle = g^{(2)}(\tau)\langle \hat{j}(t)\rangle\langle \hat{j}(t+\tau)\rangle - \left(\frac{e}{\hbar\omega}\right)\hbar\mathrm{i}\delta'(\tau)\langle \hat{j}(t)\rangle g^{(1)}(\tau), \tag{2}$$

where e indicates the electron charge, $\delta'(\tau)$ the time derivative of the Dirac delta function, $\hbar$ planck's constant, ω the light frequency and $g^{(1)}$ and $g^{(2)}$ denote the first and second order correlation function, respectively.

Furthermore, the first and second order correlation functions are related through the Siegert relationship

$$g^{(2)}(\tau) = 1 + \left|g^{(1)}(\tau)\right|^2. \tag{3}$$

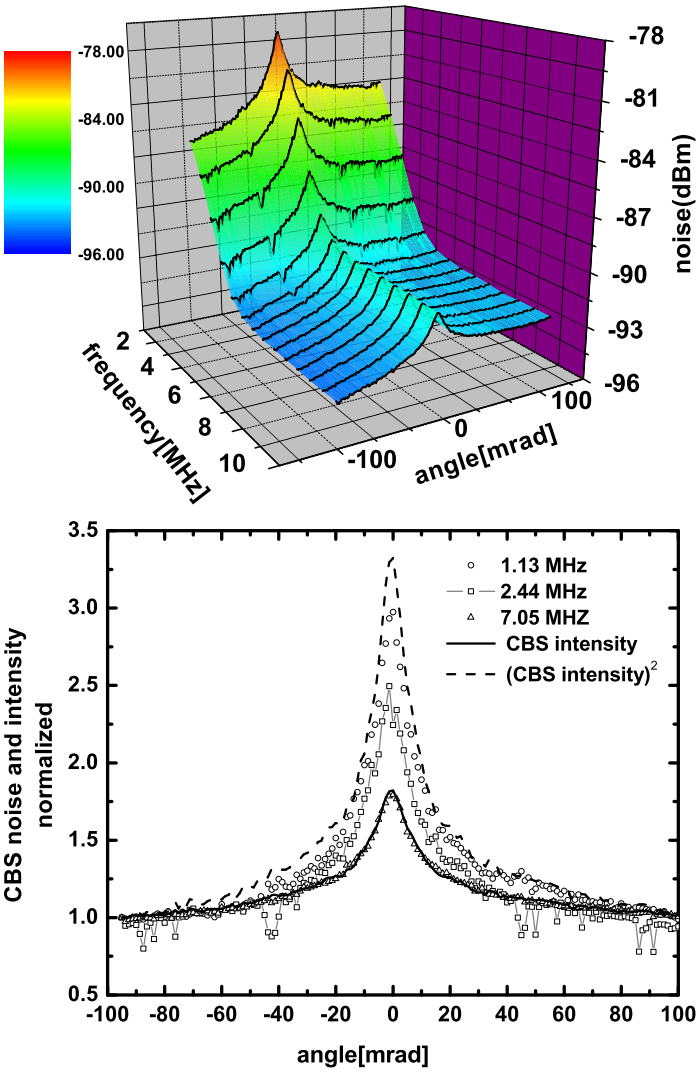

Figure 2. (top) Noise spectrum of light scattered from a gallium phosphide sample as function of backscattering angle and frequency. The CBS noise cones are clearly visible over the entire frequency range. (bottom) Comparison between CBS intensity (solid line) and CBS noise cones (symbols). At high frequency the shot noise cones match the intensity cone. As the frequency is lowered the noise cones exceed the intensity cone and approach the maximum value given by the squared intensity cone data (dashed line).

All is left to be calculated is $g^{(1)}(\tau)$. Up to now the properties of the rotating diffuser that generates pseudothermal light have not been used. The result provided by Estes *et al* [39] calculates $g^{(1)}(\tau)$ for a rotating ground glass diffuser, yielding

$$g^{(1)}(\tau) = \frac{2\pi\sigma^2}{A} \nu \overline{s^2} \exp\left(-\mathrm{i}\omega\tau - \frac{v^2\tau^2}{2}\left(\frac{k^2\sigma^2}{f^2} + \frac{1}{4\sigma^2}\right)\right). \tag{4}$$

In equation (4), and with reference to figure 1, σ^2 is the cross section of the incident beam, ν is the number of independent microareas we divide the diffuser into, A is the illuminated area

on the surface of the diffuser, v is the rotating speed of the diffuser, f is the focal length of the focusing lens and s is a term that takes into account diffraction from the microareas.

Here and in the following, $\bar{\cdot}$ indicates a classical ensemble average. By looking at equation (4) we define the coherence time τ_c of the pseudothermal source as

$$\frac{1}{\tau_c^2} \equiv \frac{v^2}{2}\left(\frac{k^2\sigma^2}{f^2} + \frac{1}{4\sigma^2}\right). \tag{5}$$

On inserting equation (2) in equation (1), and making use of equation (4) it is found that

$$\begin{aligned} S(\Omega) &= \int_{-\infty}^{+\infty} \langle \hat{j}(t)\hat{j}(t+\tau)\rangle \exp(-\mathrm{i}\Omega\tau)\,\mathrm{d}\tau \\ &= \langle \hat{j}(t)\rangle^2 \delta(\Omega) + \langle \hat{j}(t)\rangle^2 \left(\frac{\zeta}{e}\right)^2 \sqrt{2\pi}\frac{\tau_c}{2}\exp\left\{-\frac{\Omega^2\tau_c^2}{8}\right\} + \langle \hat{j}(t)\rangle\left(\frac{\omega+\Omega}{\omega}\right)\zeta \end{aligned} \tag{6}$$

with

$$\zeta = e\frac{2\pi\sigma^2 v\overline{s^2}}{A}. \tag{7}$$

The first part of equation (6) contains a delta function that represents the dc component of the spectrum. The second part of equation (6) contains a frequency-dependent Gaussian spectrum which scales quadratically with the intensity. This term is the classical noise contribution originating from the fluctuations introduced by the rotating ground glass. Finally the third part of equation (6) displays a flat, frequency independent term because, given the experimental conditions ($\omega \gg \Omega$), the frequency ratio yields one. This term is the shot noise contribution.

The measured photocurrent is related to the light intensity by $\langle j\rangle = \gamma\langle I\rangle$ where $\langle\rangle$ is the intensity and γ a constant proportional to the responsivity of the APD detector.

In order to further the analysis we model our scattering system as a waveguide with disorder. This model implies that the number of modes supported by the waveguide is finite and gives rise to a discrete mode theory [40]. These modes, often named channels, can be associated to the direction of the light that impinges on the scattering medium and the direction of the light that is reflected by it. By adopting a waveguide geometry we can write

$$\overline{\langle I_{ab}\rangle} = \overline{R}_{ab}\langle I_a\rangle, \tag{8}$$

$$\overline{\langle I_{ab}\rangle^2} = \overline{R^2}_{ab}\langle I_a\rangle^2, \tag{9}$$

where $\overline{R}_{ab}$ indicates the classical reflection coefficient from incoming channel a to outgoing channel b, averaged over different realizations of the disorder (ensemble average). The backscattering angle is thus the angle comprised between the directions identified by incoming channel a and reflected channel b. By inserting equations (8) and (9) in equation (6) and performing ensemble average it is obtained for the ac noise spectrum

$$\overline{\langle S(\Omega)_{ab}\rangle} = \phi\overline{R}_{ab}\langle I_a\rangle + \gamma^2\overline{R^2}_{ab}\langle I_a\rangle^2\left(\frac{\zeta}{e}\right)^2\sqrt{2\pi}\left(\frac{\tau_c}{2}\right)\exp\left(-\frac{\Omega^2\tau_c^2}{8}\right), \tag{10}$$

where we have highlighted the dependence of the photocurrent spectrum on the outgoing channel b and $\phi = \gamma\zeta$. As it is seen from equation (10) the noise power spectrum has a linear dependence with respect to the intensity at high frequencies, while it is dominated by a quadratic intensity dependence at low frequencies. These different dependences determine the higher than

two enhancement factor shown at low frequency in figure 2, and the fact that the square of the CBS intensity cone is an upper bound for the CBS noise cones.

The frequency-dependent noise spectrum can be used to calculate a frequency-dependent Fano factor F defined as the ratio of the photocurrent fluctuation over the average photocurrent,

$$F(\Omega)_{ab} \equiv \frac{\overline{\langle S(\Omega)_{ab}\rangle}}{\phi \overline{R}_{ab}\langle I_a\rangle}. \tag{11}$$

In order to analyze the effect of CBS on the Fano factor, we analyze the Fano factor as a function of scattering angle and frequency.

The instrumental response is divided out by normalizing both the average intensity and the noise spectra to those of the polarization non-conserving channel, in which the CBS effect is absent. We define a Fano factor CBS enhancement $\eta_{ab}(\Omega)$ as the ratio of the normalized noise spectra to the normalized intensity

$$\eta_{ab}(\Omega) \equiv \frac{\overline{\langle S(\Omega)^{\mathrm{pc}}_{ab}\rangle}}{\langle S(\Omega)^{\mathrm{pnc}}_{ab}\rangle}\left(\frac{\overline{\langle I^{\mathrm{pc}}_{ab}\rangle}}{\langle I^{\mathrm{pnc}}_{ab}\rangle}\right)^{-1}. \tag{12}$$

Here the superscripts pc and pnc were introduced to define the polarization conserving and non-conserving backscattering channels, respectively. By expanding equation (12) we obtain

$$\eta_{ab}(\Omega) = \frac{1+\overline{R^2_{ab}}^{\mathrm{pc}}\left(\overline{R}^{\mathrm{pc}}_{ab}\right)^{-1}\langle I_a\rangle\frac{\zeta\gamma}{e^2}\sqrt{2\pi}\left(\frac{\tau_c}{2}\right)\exp\left(-\frac{\Omega^2\tau_c^2}{8}\right)}{1+\overline{R^2_{ab}}^{\mathrm{pnc}}\left(\overline{R}^{\mathrm{pnc}}_{ab}\right)^{-1}\langle I_a\rangle\frac{\zeta\gamma}{e^2}\sqrt{2\pi}\left(\frac{\tau_c}{2}\right)\exp\left(-\frac{\Omega^2\tau_c^2}{8}\right)}. \tag{13}$$

A 3D plot of the experimental Fano factor enhancement $\eta_{ab}(\Omega)$ is shown in figure 3, along with cross cuts produced for representative noise frequencies, as function of the backscattering angle. The Fano factor enhancement is 1 outside the CBS cone, as here the polarization conserving and non-conserving channels yield the same noise and intensity. Furthermore, no angular dependence is displayed in the full shot noise regime at high frequencies. The interference effect responsible for the CBS cone, as the low-frequency regime is approached, reflects itself on the development of an angular dependent Fano factor. A gradual transition as function of frequency between the 'pure' shot-noise and pseudothermal noise cases is also evident. Spiked values of $\eta_{ab}(\Omega)$ below 1 in figure 3 are due to spurious fluctuations caused by the operating stability of the laser and will be discarded in further analysis.

It is interesting to consider the situation on backscattering, by calculating $\eta_{aa}(\Omega)$ and, since in the polarization non-conserving case the CBS effect is absent, we assume

$$\frac{\overline{R^2_{aa}}^{\mathrm{pnc}}}{\overline{R}^{\mathrm{pnc}}_{aa}} = \frac{\overline{R^2_{ab}}}{\overline{R}_{ab}}. \tag{14}$$

From now on we drop the subscripts pc and pnc, as the term R_{aa} will always be referred to the polarization conserving case. We proceed by first neglecting mesoscopic effects. These effects become of importance when the photonic strength of the system is strong ($k_0\ell_{\mathrm{B}} \simeq 1$), and light that propagates along multiple scattering paths in the system undergoes interference effects. In our system it is $k_0\ell_{\mathrm{B}} \gg 1$, therefore we expect mesoscopic effects to be negligible [41]. In the

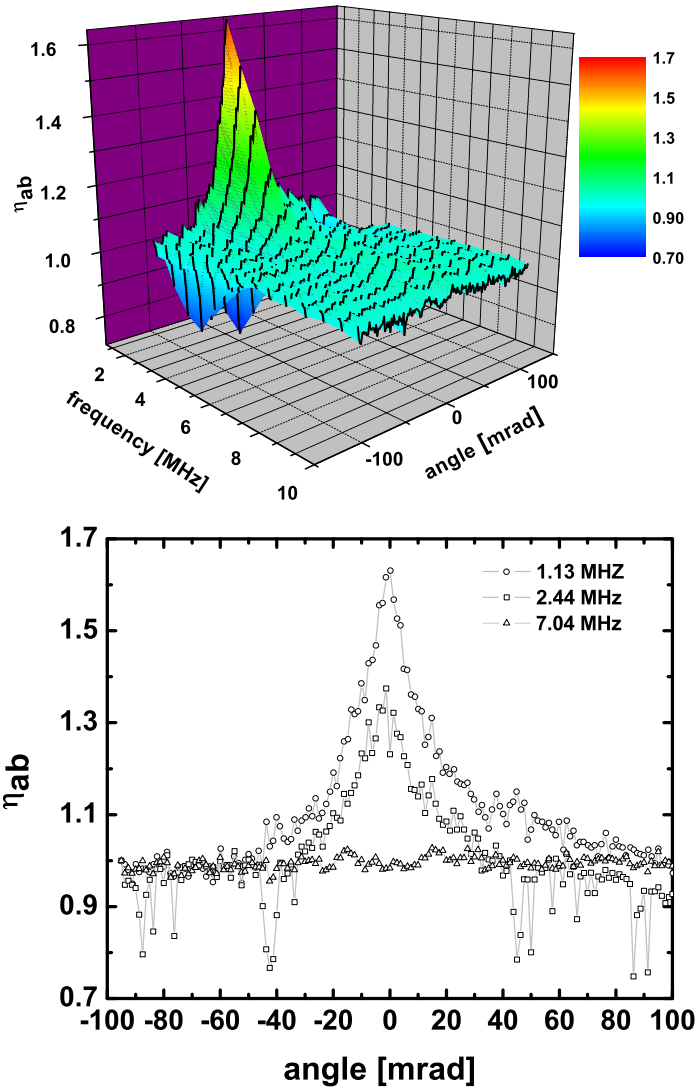

Figure 3. (top) 3D plot for the measured Fano factor CBS enhancement $\eta_{ab}(\Omega)$ as function of frequency and angle. A gallium phosphide sample with $k_0\ell_B \simeq 17.7$ has been used. The plotted data have been obtained from the raw data by binning 50 consecutive data points along the frequency axis. $\eta_{ab}(\Omega)$ varies from 1 at high frequencies in the shot noise regime to a maximum value which is always lower than the intensity CBS enhancement. Values of $\eta_{ab}(\Omega)$ below 1 are due to spurious fluctuations. (bottom) Noise CBS enhancement factor η_{ab} as function of the scattering angle around the backscattering direction at three different frequencies.

absence of mesoscopic effects the reflection coefficients obey Rayleigh statistics [42], and we have

$$\overline{R_{ab}^2} = 2\overline{R}_{ab}^2. \tag{15}$$

On backscattering it is $\overline{R}_{aa} = 2\overline{R}_{ab}$. In our experiment single scattering events and stray light contribute to making the enhancement factor for the CBS-cone lower than 2. Therefore on

backscattering we assume $\overline{R}_{aa} = (2-\beta)\overline{R}_{ab}$, with $0 < \beta < 1$. By using equations (13)–(15), the Fano factor enhancement on the backscattering direction is obtained as

$$\eta_{aa}(\Omega) = 1 + \frac{2\,(1-\beta)\left(\frac{\tau_c}{2}\right)\exp\left(-\frac{\Omega^2\tau_c^2}{8}\right)}{\alpha + 2\left(\frac{\tau_c}{2}\right)\exp\left(-\frac{\Omega^2\tau_c^2}{8}\right)} \tag{16}$$

with $\alpha = e^2(\langle I_a\rangle \overline{R}_{ab}\gamma\zeta\sqrt{2\pi})^{-1}$. The enhancement η_{aa} depends on the balance of quantum and classical noise, respectively, given by α and the exponential term in equation (16), with the frequency Ω gauging the two regimes. The behavior of η_{aa} at low and high frequency, in the classical and shot noise regimes, is given, respectively, by

$$\eta_{aa}(\Omega)_{\Omega\longrightarrow 0} = 1 + \frac{2(1-\beta)\frac{\tau_c}{2}}{2\frac{\tau_c}{2}+\alpha} \tag{17}$$

and

$$\eta_{aa}(\Omega)_{\Omega\longrightarrow \infty} = 1. \tag{18}$$

In the low-frequency limit, $\eta_{aa}(\Omega)$ approaches the CBS enhancement for the intensity, $2-\beta$. The Fano factor at high frequencies, i.e. for the coherent state, is not modified by CBS. The factor $\eta_{aa}(\Omega)$ is plotted in figure 4 (top panel) as function of noise frequency and is fitted by using equation (16). A good agreement is recovered. We note that the coherence time of our pseudothermal source τ_c is of the order of microseconds while the transport time, i.e. the time light travels one mean free path $\ell_B \simeq 2.2\,\mu$m, is of the order of femtoseconds.

Although the current experimental parameters are not in the range were mesoscopic interference is to be expected, we proceed to assess the effect of mesoscopic contributions in the CBS of noise. In order to do that we consider the first order mesoscopic contribution in the reflectivity as obtained in [43]. By exploiting equation (15) in [43] we have

$$\overline{R_{ab}^2} = \overline{R}_{ab}^2\left(2 - \frac{2}{N(1-\frac{\ell}{L})}\right) \tag{19}$$

and

$$\overline{R_{aa}^2} = \overline{R}_{aa}^2\left(2 - \frac{3}{N(1-\frac{\ell}{L})}\right), \tag{20}$$

where N is the number of channels.

The dimensionless conductance g, defined in transmission, is given by Akkermans and Montambaux [42]

$$g = \frac{N\ell}{L}. \tag{21}$$

In reflection, following the same procedure as the one adopted for g we define

$$g_r \equiv \sum_{a,b}\overline{R}_{ab}. \tag{22}$$

and, using the fact that $\overline{R}_{ab} = \frac{1}{N}(1-\frac{\ell}{L})$ it is found

$$g_r = N\left(1 - \frac{\ell}{L}\right). \tag{23}$$

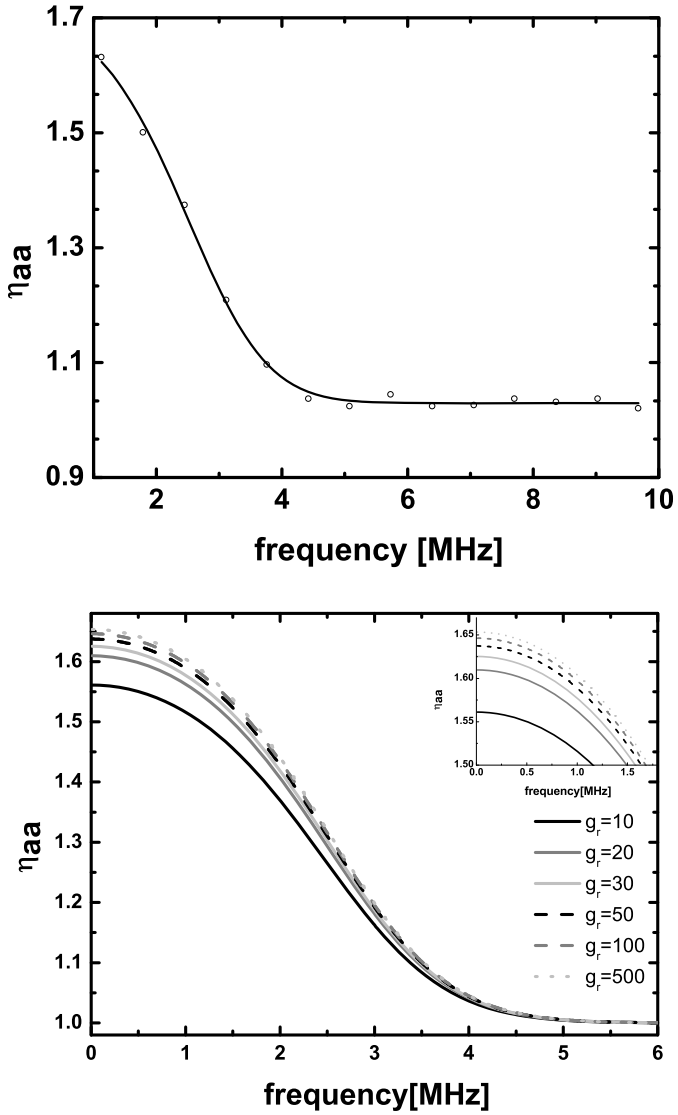

Figure 4. (top) Observed noise CBS enhancement factor on backscattering η_{aa} as function of frequency. The enhancement factor $\eta_{aa}(\Omega)$ has been obtained by taking the maximum of $\eta_{ab}(\Omega)$ at each frequency. The solid line is a fit of the theoretical lineshape for η_{aa}, equation (16), to the data with α, β and τ_c as fit parameters. (bottom) Calculations that illustrate the effect of g_r on $\eta_{aa}(\Omega)$. Low g_r values induce stronger variations, especially at low frequencies. As g_r increases η_{aa} quickly converges towards the limit function in equation (16) and deviations caused by high g_r values become difficult to be discerned. The inset highlights the different values reached by η_{aa} at $\Omega = 0$. In the shown calculation the parameters α, β and τ_c have been assigned the values obtained by fitting the data to the lineshape for η_{aa} when mesoscopic effects are negligible.

Formulae (19) and (20) express the fact that when g_r^{-1} contributions are negligible the reflected intensity follows a Rayleigh distribution. Deviations from Rayleigh statistics arise in the mesoscopic regime, when interferences effect between multiple scattering paths start to play a role.

By using equations (13), (19) and (20), the Fano factor enhancement on the backscattering direction is obtained as

$$\eta_{aa}(\Omega) = 1 + \frac{\left[2(1-\beta)\left(1-g_r^{-1}\right) - (2-\beta)\,g_r^{-1}\right]\left(\frac{\tau_c}{2}\right)\exp\left(-\frac{\Omega^2\tau_c^2}{8}\right)}{\alpha + 2\left(1-g_r^{-1}\right)\left(\frac{\tau_c}{2}\right)\exp\left(-\frac{\Omega^2\tau_c^2}{8}\right)}. \tag{24}$$

In figure 4 (bottom panel) the effect of a selection of g_r values on η_{aa} is shown. The Fano factor CBS enhancement η_{aa} is sensitive to a broad range of g_r values. This is due to the quadratic dependence of the excess noise on the intensity at low frequencies and to the constructive interference between direct and reverse paths characteristic of backscattering that manifests itself in the difference between equations (19) and (20). These properties of η_{aa} offer the possibility to investigate mesoscopic correlations and gather information about light transport in proximity of Anderson localization.

4. Conclusion

In conclusion we have shown for the first time photon noise measurements in the weak localization regime, and have shown that the transition from the full shot noise regime at high frequency to the full pseudothermal domain at low frequency can be experimentally investigated. We have experimentally demonstrated the enhancement of the Fano factor around the backscattering direction due to the CBS effect. By calculating the first order mesoscopic correction, we find that the enhancement of the Fano factor CBS depends on the number of open reflection channels g_r^{-1}. The standard intensity CBS cone does not have this correction whereas measuring photon noise gives access to $\overline{R^2}_{ab}$, from which the magnitude of g_r^{-1} effects could in principle be extracted. More specifically, our approach indicates that the enhancement displayed by the noise cone reveals information about mesoscopic correlations. These correlations give rise to deviations from Rayleigh statistics in the strongly scattering regime [44]. The use of the CBS technique has in addition the potential to study the first and second moment of the probability distribution as function of the path length.

Our experiments show for the first time that sensitive photon noise experiments can be combined with CBS, opening up new avenues for studying quantum optical aspects of diffuse wave transport. Future experiments on photon noise in the strong scattering regime may be performed to explore mesoscopic quantum corrections and localization. Noise measurements could prove themselves useful also in systems that display gain, random lasing and absorption [16, 45–47]. Furthermore, the impact of Anderson localization on non-classical properties of light is yet an open question and is a new and exciting field [48, 49].

References

[1] Sheng P 1995 *Introduction to Wave Scattering, Localization and Mesososcopic Phenomena* ed S Diego (New York: Academic)
[2] Albada M P V and Lagendijk A 1985 *Phys. Rev. Lett.* **55** 2692
[3] Wolf P E and Maret G 1985 *Phys. Rev. Lett.* **55** 2696
[4] Chabanov A A and Genack A Z 2001 *Phys. Rev. Lett.* **87** 233903
[5] Scheffold F and Maret G 1998 *Phys. Rev. Lett.* **81** 5800
[6] Cao H 2003 *Waves Random Media* **13** R1

[7] Garcia P D, Stobbe S, Sallner I and Lodahl P 2012 *Phys. Rev. Lett.* **109** 253902
[8] Sperling T, Buhrer W, Aegerter C M and Maret G 2013 *Nature Photon.* **7** 48
[9] Storzer M, Gross P, Aegerter C M and Maret G 2006 *Phys. Rev. Lett.* **96** 063904
[10] Strudley T, Zehender T, Blejean C, Bakkers E P A M and Muskens O L 2013 *Nature Photon.* **7** 413
[11] Oberholzer S, Sukhorukov E V and Schonenberger C 2002 *Nature* **415** 765
[12] Oberholzer S, Bieri E, Schönenberger C, Giovannini M and Faist J 2006 *Phys. Rev. Lett.* **96** 046804
[13] Henny M, Oberholzer S, Strunk C and Schönenberger C 1999 *Phys. Rev.* B **59** 2871
[14] Lodahl P, Mosk A P and Lagendijk A 2005 *Phys. Rev. Lett.* **95** 173901
[15] Lodahl P and Lagendijk A 2005 *Phys. Rev. Lett.* **94** 153905
[16] Patra M and Beenakker C W J 2000 *Phys. Rev.* A **61** 063805
[17] Beenakker C W J 1998 *Phys. Rev. Lett.* **81** 1829
[18] Smolka S, Huck A, Andersen U L, Lagendijk A and Lodahl P 2009 *Phys. Rev. Lett.* **102** 193901
[19] Schlawin F, Cherroret N and Buchleitner A 2012 *Europhys. Lett.* **99** 14001
[20] Cherroret N and Buchleitner A 2011 *Phys. Rev.* A **83** 033827
[21] Canda M and Skipetrov S E 2013 *Phys. Rev.* A **87** 013846
[22] Skipetrov S E 2007 *Phys. Rev.* A **75** 053808
[23] Balog S, Zakharov P, Scheffold F and Skipetrov S 2006 *Phys. Rev. Lett.* **97** 103901
[24] Ozbay E 2006 *Science* **311** 189
[25] Tworzydło J and Beenakker C W J 2002 *Phys. Rev. Lett.* **89** 043902
[26] Derode A, Tourin A, de Rosny J, Tanter M, Yon S and Fink M 2003 *Phys. Rev. Lett.* **90** 014301
[27] Henry C H and Kazarinov R F 1996 *Rev. Mod. Phys.* **68** 801
[28] Loudon R 2000 *The Quantum Theory of Light* (Oxford: Oxford University Press)
[29] Uchida A *et al* 2008 *Nature Photon.* **2** 728
[30] Reidler I, Aviad Y, Rosenbluh M and Kanter I 2009 *Phys. Rev. Lett.* **103** 024102
[31] Koenderink A F, Megens M, van Soest G, Vos W L and Lagendijk A 2000 *Phys. Lett.* A **268** 104
[32] Kim Y L, Liu Y, Turzhitsky V M, Roy H K, Wali R K and Backman V 2004 *Opt. Lett.* **29** 1906
[33] Muskens O L and Lagendijk A 2008 *Opt. Express* **16** 1222
[34] Anderson P W 1958 *Phys. Rev.* **109** 1492
[35] Wiersma A L D S, Bartolini P and Righini R 1997 *Nature* **390** 671
[36] Scheffold F, Lenke R, Tweer R and Maret G 1999 *Nature* **398** 206
[37] Schuurmans F, Vanmaekelbergh D, Van De Lagemaat J and Lagendijk A 1999 *Science* **284** 141
[38] Ben-Aryeh Y and Huttner B 1987 *Phys. Rev.* A **36** 1249
[39] Estes L E, Narducci L M and Tuft R A 1971 *J. Opt. Soc. Am.* **61** 1301
[40] Beenakker C W J 1997 *Rev. Mod. Phys.* **69** 731
[41] van Rossum M C W and Nieuwenhuizen T M 1999 *Rev. Mod. Phys.* **71** 313
[42] Akkermans E and Montambaux G 2007 *Mesoscopic Physics of Electrons and Photons* (Cambridge: Cambridge University Press)
[43] Mello P A, Akkermans E and Shapiro B 1988 *Phys. Rev. Lett.* **61** 459
[44] Muskens O L, van der Beek T and Lagendijk A 2011 *Phys. Rev.* B **84** 035106
[45] Patra M and Beenakker C W J 1999 *Phys. Rev.* A **60** 4059
[46] Kindermann M, Nazarov Y V and Beenakker C W J 2002 *Phys. Rev. Lett.* **88** 063601
[47] Fedorov V Y and Skipetrov S E 2009 *Phys. Rev.* A **79** 063822
[48] Ott J R, Mortensen N A and Lodahl P 2010 *Phys. Rev. Lett.* **105** 090501
[49] Crespi A, Osellame R, Ramponi R, Giovannetti V, Fazio R, Sansoni L, De Nicola F, Sciarrino F and Mataloni P 2013 *Nature Photon.* **7** 322